Topics in Catalysis (2019) 62:214–218
https://doi.org/10.1007/s11244-018-1085-0

ORIGINAL ARTICLE

Hydrothermal Synthesis of Titanate Nanotubes with Different Pore Structure and its Effect on the Catalytic Performance of V_2O_5-WO_3/Titanate Nanotube Catalysts for NH_3-SCR

Inhak Song[1] · Hwangho Lee[1] · Se Won Jeon[1] · Dong-ha Lim[2] · Do Heui Kim[1]

Published online: 2 November 2018

Abstract
In this work, titanate nanotubes (TNT) with different pore structure were synthesized through hydrothermal method by using various TiO_2 particles as starting materials. V_2O_5 and WO_3 was deposited on the as-synthesized TNT structure by wet impregnation. In the selective catalytic reduction of NO with NH_3, it was found that the catalytic activity of V_2O_5-WO_3/TNT catalysts was unaffected by the initial different pore structure because the pore structure collapsed during the active metal impregnation and subsequent calcination. Also, kinetic analysis showed that the apparent activation energies of V_2O_5-WO_3/TNT catalysts and traditional V_2O_5-WO_3/TiO_2 catalyst were the similar values, which indicate that the nature of active sites in the SCR reaction on both catalysts would not be significantly different.

Keywords V_2O_5-WO_3/TiO_2 · TiO_2 nanotube · Selective catalytic reduction · Pore structure · DeNOx

1 Introduction

Selective catalytic reduction (SCR) reaction is a well-known technology to remove NO_x by using NH_3 as reducing agent [1]. The most commercially available catalyst is vanadium based catalysts, which shows high SCR activity in the middle temperature range (300–400 °C). In general, the commercial catalysts consist of 1–2 wt% of V_2O_5 and 8–10 wt% of WO_3 dispersed on anatase TiO_2(101) support [2]. Tungsten oxides are usually added to promote catalytic activity of V and to increase thermal stability of vanadium based catalysts. The biggest advantage of vanadium catalysts is their strong sulfur resistance, which allows SCR operation in combustion engines using fuel with high sulfur content [3]. In industrial applications, it is important to put a large amount of active metal in a limited space to enhance catalytic performance. Thus, many research groups have focused on the optimization of SCR active site by morphological change of TiO_2 supports [4–6].

It is well known that titanate nanotubes with high surface area can be easily prepared by hydrothermal synthesis in the alkali solution [7]. Recently, various active metal oxides supported on the titanate nanotube (TNT) have been used in the NH_3-SCR reaction. Xiong et al. prepared TiO_2 nanotube-supported V_2O_5 catalyst, which showed much higher deNO_x efficiency and satisfactory resistance to water and sulfur compared to raw-TiO_2 supported V_2O_5 catalyst [8]. Mejía-Centeno et al. also found that V_2O_5-WO_3/$H_2Ti_3O_7$ catalyst showed a high NO conversion at low temperature (240 °C). They suggested that the nanotube morphology can be maintained up to 480 °C [9]. Non-vanadium SCR catalysts with Mn, Ce and Cu as active materials have also been attempted using titanate nanotubes as support materials and most works have confirmed enhanced activity and selectivity of these catalysts [10–13]. In this work, various titanate nanotubes with different pore structures were prepared using various TiO_2 precursor materials and tested as a support for the V_2O_5-WO_3 catalyst in SCR reaction.

✉ Do Heui Kim
dohkim@snu.ac.kr

[1] School of Chemical and Biological Engineering, Institute of Chemical Processes, Seoul National University, Seoul 08826, Republic of Korea

[2] Offshore Plant Resources R&D Center, Korea Institute of Industrial Technology, Busan 46938, Republic of Korea

2 Experimental

2.1 The Preparation of Catalysts

Titanate nanotube (TNT) was synthesized by conventional hydrothermal synthesis. Specifically, 3 g of TiO_2 powder (DT51, P25, Sigma) was added to 10 M NaOH solution and mixed vigorously in a Teflon lined autoclave. White slurry in the autoclave was heated at 150 °C for 24 h under static condition. After cooling down to the room temperature, the slurry was filtered with 3 L of 0.2 M HCl solution and subsequently washed with 3 L of distilled water. The obtained white powder was dried at 105 °C overnight, which was designated by the name of its precursor TiO_2 powder (ex. TNT-DT51). As-synthesized TNT was impregnated with ammonium metavanadate (NH_4VO_3) and ammonium metatungstate ($(NH_4)_6H_2W_{12}O_{40}$) dissolved in oxalic acid solution. The samples were dried at 105 °C and calcined at 500 °C for 4 h in air condition. The V_2O_5 and WO_3 contents of catalysts were 3 wt% and 10 wt%, respectively. Prepared catalysts were designated as VW/the type of TNT.

2.2 Characterization Techniques

The morphological properties of samples were observed with a field emission scanning electron microscope (JSM-6360 (JEOL)) with the accelerating voltage of 20 kV, and the samples were coated with Pt metal with MSC-101 (JEOL) before measurements. N_2 adsorption & desorption isotherms were obtained by using ASAP 2010 apparatus of Micromeritics. BET surface areas were calculated in the P/P_0 range of 0.05–0.20. X-ray diffraction patterns were obtained by using Ultra X18 (Rigaku) with a Cu Kα radiation, and the patterns were normally recorded with the step size of 0.02° at the scan speed of 5°/min. A series of Raman spectra were obtained using 532 nm laser excitation on DXR2xi (Thermo, USA) Raman spectrometer at NCIRF (National Center for Inter-university Research Facilities, Seoul National University, Korea).

2.3 Measurements of Catalytic Activity

The standard selective catalytic reduction (SCR) reaction was carried out in a fixed bed tubular reactor with a diameter of half inch. Normally, 0.12 g of the catalyst particles sieved in the size of 180–250 μm were used, and the total flow rate of the simulated exhaust gas was 200 mL min^{-1}. The inlet concentration of the reactants was 500 ppm NO, 500 ppm NH_3, 10% O_2, 10% H_2O, 5% CO_2 balanced with N_2. Space velocity of the reaction system was determined to be 100,000 mL $g^{-1}{\cdot}h^{-1}$. The reaction temperature was increased from 100 to 450 °C with 50 °C intervals and the activity was measured at steady state. NO_x chemiluminescence analyzer (42i High level, Thermo Scientific) was utilized to measure NO_x concentration of outlet gas. Fourier transform infrared spectroscopy (FT-IR) equipped with a 2 m gas cell was used to measure the concentration of N_2O. NO_x conversion was calculated by using the following equation.

$$NO_x \ \ conversion \ \ (\%) = \frac{\left[NO_x\right]_{in} - \left[NO_x\right]_{out}}{\left[NO_x\right]_{in}} \times 100$$

In kinetic analysis, the internal and external mass transfer effects were neglected below 250 °C. The differential equation was derived using the previously reported plug flow reactor model as follows [14]:

$$\ln(-\ln(1-x)) = -\frac{E'}{R}\frac{1}{T} + \ln\left(\frac{P}{FR}V_{cat}A'\right)$$

where x is the NO fractional conversion; F is the total gas molar flow rate; V_{cat} is the catalyst volume; R is the ideal gas constant; P is the total pressure; T is the temperature; E' is the apparent activation energy; A' is the pre-exponential factor. The apparent activation energy was calculated by linear fitting between $1/T$ and $\ln(-\ln(1-x))$.

3 Results and Discussion

The morphology of TiO_2 (P25) before and after hydrothermal treatment was shown in Fig. 1. The initial TiO_2 particles have a spherical morphology of 30–40 nm diameter, and individual particles have been observed to aggregate to form large particles. After hydrothermal treatment in 10 M NaOH solution and subsequent HCl washing, long and thin tubular particles were obtained. Each tube has a diameter of 15–20 nm and a length of several hundred nm. It can be seen that the nanotubes are randomly entangled to form large aggregates. Since the tube is hollowed, the nanotube itself has a pore structure with an inner diameter about 10 nm. In addition, the external space between nanotubes present in the nanotube aggregates can also contribute to the porous structure.

The various kind of TiO_2 particles (DT51, P25, Sigma) were used to synthesize TNT in the same condition. As-synthesized TNTs were dried at 100 °C in air, and pretreated in vacuum condition to eliminate water inside the pore before BET analysis. N_2 adsorption desorption curves of prepared TNTs were shown in Fig. 2. It was confirmed that TNTs with a large pore volume were successfully synthesized regardless of the type of raw TiO_2 particles (Table 1). However, the pore volume, size or BET surface area of each TNT were slightly different from each other. For example, TNT-DT51

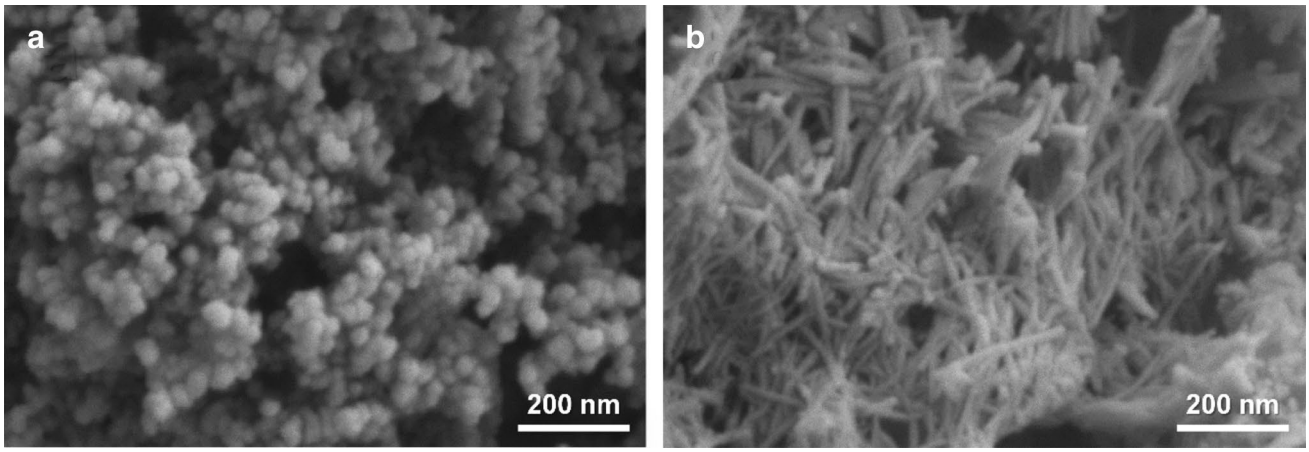

Fig. 1 Field emission SEM images of **a** the starting TiO_2 particle (P25), and **b** the as-synthesized TNT

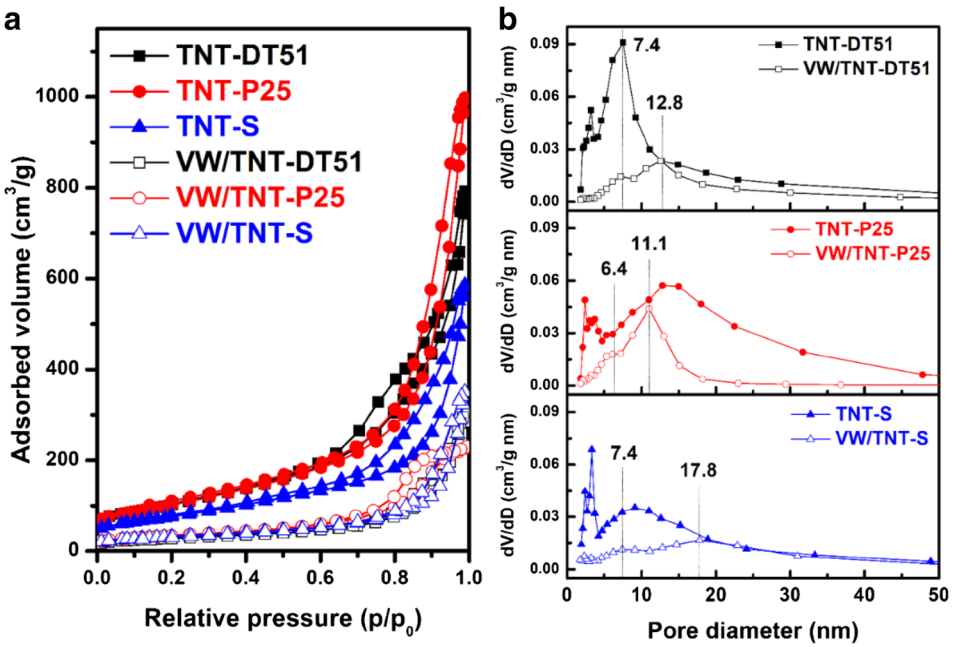

Fig. 2 **a** N2 adsorption and desorption curves and **b** BJH pore size distribution curves of the prepared various TNT and VW/TNT catalysts

and TNT-P25 have similar surface areas of 360 m^2/g, but TNT-P25 has a much larger pore volume and size than TNT-DT51. In the case of TNT-S, surface area and pore volume are much smaller than others. It seems that the initial size and morphology of TiO_2 particle can affect the degree of entanglement of nanotubes in hydrothermal synthesis. The tight and dense entanglement of nanotubes can make the small void between nanotube networks.

It is necessary to investigate the pore collapse property of nanotube structures which occurs mainly after the impregnation of the active metal oxide and subsequent calcination process. The collapse of pore structure is an important factor because it can reduce the number of exposed active sites and reduce the reaction rate, and the reduction of surface area can lead to sintering of the dispersed active metal oxide. In this experiment, 3 wt% V_2O_5 and 10 wt% WO_3 are loaded on TNTs and calcined at 500 °C for 4 h in air condition. The changes of pore structure of various VW/TNT catalysts were analyzed and shown in Fig. 2. The common feature of the three kinds of VW/TNTs is the total collapse of small pores less than 3 nm. Also, it can be seen that pore size distribution curves shifted to large pore size region for all cases, which can be attributed to shrinkage of nanotube aggregates. Thus, at least in this case, the inner surface of nanotubes with small diameter can no longer function as valid surface area for dispersed V or W active sites after calcination at 500 °C. Regardless of initial morphology of TNTs, pore volume and surface area of VW/TNT catalysts are all similar each other

Table 1 Textural properties of the prepared TNT, VW/TNT and VW/TiO_2 catalysts

Sample	S_{BET} (m^2g^{-1-1})[a]	V_{pore} (cm^3g^{-1})[b]	Average pore size (nm)
TNT-DT51	364	0.98	10.7
TNT-P25	363	1.31	14.4
TNT-S	270	0.73	10.8
TiO_2(DT51)	83	0.29	14.0
VW/TNT-DT51	100	0.36	14.5
VW/TNT-P25	121	0.34	11.2
VW/TNT-S	114	0.40	14.1
VW/TiO_2(DT51)	74	0.26	13.8

[a]BET surface areas were measured in the P/P_0 range of 0.05–0.20

[b]Pore volumes were calculated at $P/P_0 = 0.97$

as shown in Table 1. Hence, it seems difficult to maintain the structural advantages of TNT after V impregnation and calcination. In the case of TiO_2(DT-51), however, it can be seen that the structural characteristics are almost same before and after V and W impregnation and calcination process.

XRD patterns of the prepared VW/TNT catalysts are shown in Fig. 3a. The sharp peak at 25.4° can be attributed to the anatase TiO_2 phase. It is known that the phase of as-synthesized TNT is titanate ($H_2Ti_3O_7$) before thermal treatment [15]. Wrapping of layered titanate leads to the formation of titanate nanotube structure. Phase transformation from titanate to anatase occurs during calcination. In the case of VW/TNT catalysts, it was confirmed that all titanate phase completely converted to the anatase phase. No peaks related to V_2O_5 or WO_3 are found except the peak of anatase phase, which indicates that V and W are well dispersed on the TNT surface. Raman spectra of the prepared VW/TNT catalysts are also shown in Fig. 3b since small nanocrystals of V_2O_5 or WO_3 might not be able to be detected on the surface by XRD. No sharp peak at 994 cm^{-1} was observed for the series of VW/TNT catalysts, which means that the nanocrystals of V_2O_5 was not formed after calcination. Meanwhile, the peak at ~800 cm^{-1} was found in all samples, indicating the presence of small nanocrystals of WO_3.

Various VW/TNT catalysts are tested in standard SCR reaction (Fig. 4a). Regardless of the type of TNT, VW/TNT catalysts exhibit similar SCR performance over the entire temperature range. N_2O selectivity was less than 1% over the whole temperature. This implies that initial pore structure of TNT cannot affect the activity of VW/TNT catalysts. Meanwhile, there is a large difference between VW/TNT series and VW/TiO_2. At low temperature below 300 °C, VW/TiO_2 exhibits much higher NO_x removal rate than VW/TNT catalysts. However, VW/TNT catalysts exhibit more stable SCR performance than VW/TiO_2 at high temperature

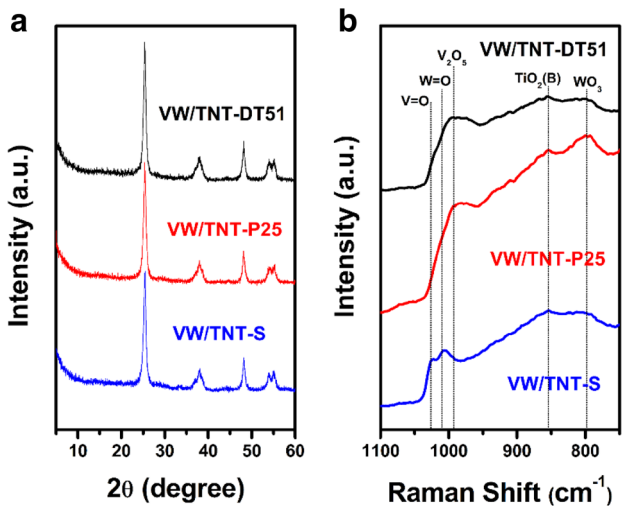

Fig. 3 **a** XRD patterns and **b** Raman spectra of the prepared VW/TNT catalysts

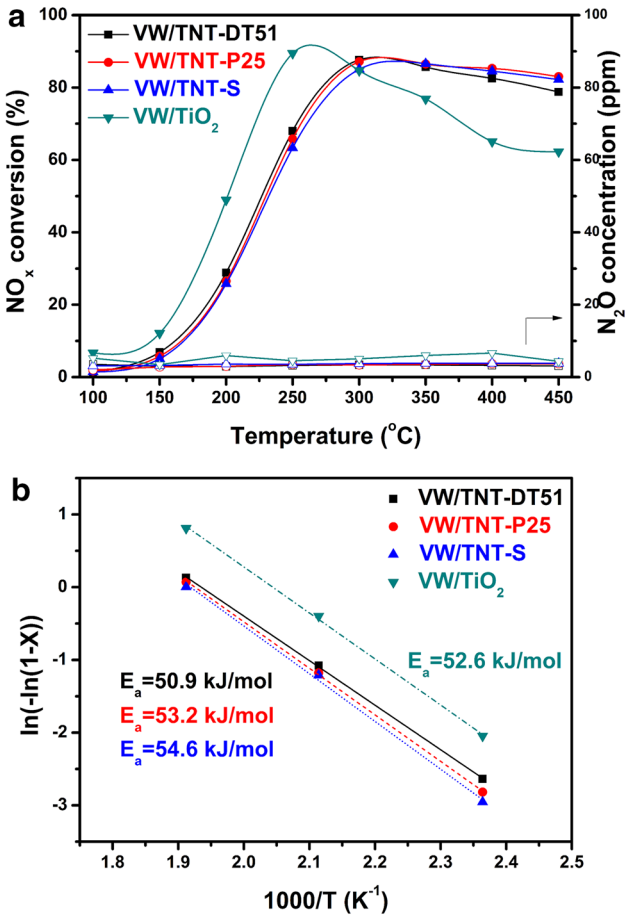

Fig. 4 Standard NH3-SCR activity over the prepared VW/TNT catalysts compared to to VW/TiO_2 catalyst. Reaction conditions: $[NO] = [NH_3] = 500$ ppm, $[O_2] = 10\%$, $[H_2O] = 10\%$, $[CO_2] = 5\%$ balanced with N_2, GHSV = 100,000 mL min^{-1} g^{-1}. **b** kinetic analysis for the tested catalysts below 250 °C

of 300–450 °C. In Fig. 4b, kinetic analysis was carried out from the NO_x conversion data in order to understand the catalytic difference of VW/TiO_2 and VW/TNT catalyst. It was assumed that the internal and external mass transfer effects can be neglected below 250 °C [16]. VW/TNT and VW/TiO_2 catalysts have quite similar standard SCR apparent activation energies in the range of 51–55 kJ/mol, which is consistent with previous report [14]. This observation indicates that the mechanistic nature of V-W active sites are nearly unchanged, and the different reaction rates of the two catalysts are due to the number of active sites. The number of active sites of VW/TNT may be less than that of VW/TiO_2 because the active metal in TNT is buried by the collapse of tube structure. Meanwhile, the decreasing activity of VW/TiO_2 at high temperatures above 300 °C is known to be due to NH_3 oxidation catalyzed by large VO_x cluster. It can be seen that the large surface area of TNT is advantageous in dispersing V sites to prevent the formation of large VO_x clusters.

In summary, TNTs with different pore structures were obtained by using various TiO_2 particles. Such difference, however, was not retained after V and W impregnation and subsequent calcination process, and the SCR performance of the various VW/TNT catalysts showed little difference. A series of VW/TNT catalysts exhibited lower NO_x removal rate than conventional VW/TiO_2, which may arise from the loss of active site by the collapse of tube structures based on the kinetic analysis. Stable SCR performance of VW/TNT catalysts at high temperature above 300 °C suggested that the advantage of using TNT is to prevent the formation of large VO_x species that are detrimental to SCR activity.

Acknowledgements The authors acknowledge the World Class 300 Project Programs (0458-20170019) funded by the Korea Institute for Advancement of Technology (KIAT) for the financial support.

References

1. Li J, Chang H, Ma L, Hao J, Yang RT (2011) Catal Today 175(1):147–156
2. Lietti L, Forzatti P, Bregani F (1996) Ind Eng Chem Res 35(11):3884–3892
3. Youn S, Song I, Lee H, Cho SJ, Kim DH (2017) Catal Today 303:19–24
4. Song I, Youn S, Lee H, Lee SG, Cho SJ, Kim DH (2017) Appl Catal B 210:421–431
5. Deng S, Meng T, Xu B, Gao F, Ding Y, Yu L, Fan Y (2016) ACS Catal 6(9):5807–5815
6. Chen X, Cao S, Weng X, Wang H, Wu Z (2012) Catal Commun 26:178–182
7. Kasuga T, Hiramatsu M, Hoson A, Sekino T, Niihara K (1998) Langmuir 14(12):3160–3163
8. Xiong L, Zhong Q, Chen Q, Zhang S (2013) Korean J Chem Eng 30(4):836–841
9. Mejía-Centeno I, Castillo S, Camposeco R, Marín J, García LA, Fuentes GA (2015) Chem Eng J 264:873–885
10. Pappas DK, Boningari T, Boolchand P, Smirniotis PG (2016) J Catal 334:1–13
11. Chen X, Wang P, Fang P, Wang H, Cen C, Zeng W, Wu Z (2017) Environ Sci Nano 4(2):437–447
12. Wang H, Chen X, Weng X, Liu Y, Gao S, Wu Z (2011) Catal Commun 12(11):1042–1045
13. Camposeco R, Castillo S, Mugica V, Mejía-Centeno I, Marín J (2014) Chem Eng J 242:313–320
14. Xi Y, Ottinger NA, Liu ZG (2014) Appl Catal B 160:1–9
15. Chen Q, Zhou W, Du GH, Peng LM (2002) Adv Mater 14(17):1208–1211
16. Guo X, Bartholomew C, Hecker W, Baxter LL (2009) Appl Catal B 92(1–2):30–40